THE JOURNAL OF BIOLOGICAL CHEMISTRY VOL. 291, NO. 49, pp. 25306–25318, December 2, 2016

Exercise Inducible Lactate Dehydrogenase B Regulates Mitochondrial Function in Skeletal Muscle*

Received for publication, July 25, 2016, and in revised form, October 1, 2016 Published, JBC Papers in Press, October 13, 2016, DOI 10.1074/jbc.M116.749424

Xijun Liang[‡1], Lin Liu[‡1], Tingting Fu[‡], Qian Zhou[‡], Danxia Zhou[‡], Liwei Xiao[‡], Jing Liu[‡], Yan Kong[§], Hui Xie[¶], Fanchao Yi[¶], Ling Lai[‖], Rick B. Vega[‖], Daniel P. Kelly[‖], Steven R. Smith[¶], and Zhenji Gan[‡2]**

*From the [‡]State Key Laboratory of Pharmaceutical Biotechnology and Ministry of Education Key Laboratory of Model Animals for Disease Study, Model Animal Research Center of Nanjing University, Nanjing 210061, China, the [§]Department of Biochemistry and Molecular Biology, School of Medicine, Southeast University, Nanjing 210009, China, the [¶]Translational Research Institute for Metabolism and Diabetes, Florida Hospital, Orlando, Florida 32804, the [‖]Diabetes and Obesity Research Center, Sanford Burnham Prebys Medical Discovery Institute, Orlando, Florida 32827, and the **Collaborative Innovation Center of Genetics and Development, Shanghai 200438, China*

Edited by Jeffrey Pessin

Lactate dehydrogenase (LDH) catalyzes the interconversion of pyruvate and lactate, which are critical fuel metabolites of skeletal muscle particularly during exercise. However, the physiological relevance of LDH remains poorly understood. Here we show that *Ldhb* expression is induced by exercise in human muscle and negatively correlated with changes in intramuscular pH levels, a marker of lactate production, during isometric exercise. We found that the expression of *Ldhb* is regulated by exercise-induced peroxisome proliferator-activated receptor γ coactivator 1α (PGC-1α). *Ldhb* gene promoter reporter studies demonstrated that PGC-1α activates *Ldhb* gene expression through multiple conserved estrogen-related receptor (ERR) and myocyte enhancer factor 2 (MEF2) binding sites. Transgenic mice overexpressing *Ldhb* in muscle (muscle creatine kinase (MCK)-Ldhb) exhibited increased exercise performance and enhanced oxygen consumption during exercise. MCK-Ldhb muscle was shown to have enhanced mitochondrial enzyme activity and increased mitochondrial gene expression, suggesting an adaptive oxidative muscle transformation. In addition, mitochondrial respiration capacity was increased and lactate production decreased in MCK-Ldhb skeletal myotubes in culture. Together, these results identified a previously unrecognized *Ldhb*-driven alteration in muscle mitochondrial function and suggested a mechanism for the adaptive metabolic response induced by exercise training.

Muscle fitness and resistance to fatigue depend strongly on the capacity to burn the fuels, including fatty acids and glucose, to meet ATP demands (1–5). Exercise training is effective in improving muscle fitness by promoting favorable muscle metabolic reprograming including capacity for fuel burning, mitochondrial ATP production, and contraction (6–13). Conversely, many chronic diseases, including obesity, diabetes, muscular diseases, and aging, are associated with decreased muscle fitness, contributing to a vicious cycle of inactivity and further promoting the progression of chronic diseases (6–8, 11, 12, 14). Thus, a better understanding of the molecular regulatory pathways involved in the beneficial effects of exercise training on muscle fuel metabolism could yield novel therapeutic targets aimed at the prevention or treatment of diseases associated with muscle bioenergetics defects.

The molecular and cellular mechanisms of skeletal muscle adaptation to exercise training are unclear. Exercise training-induced adaptations in skeletal muscle are reflected, in part, by changes in transcriptional response and metabolite flux (1, 2, 4, 5, 11, 15, 16). Previous studies have demonstrated that the PGC-1α[3] transcriptional regulatory circuit, including the nuclear receptors PPAR and ERR, is a key transducer of exercise-responsive gene expression. The PGC-1α circuit regulates a broad array of genes involved in mitochondrial biogenesis and fuel metabolism (17–25). Evidence is also emerging that manipulation of metabolic enzyme or metabolite flux in skeletal muscle can significantly affect muscle performance and resistance to fatigue (26, 27). We are just beginning to explore the physiological relevance of metabolic enzyme activation and metabolite flux alterations in regulating muscle function.

Pyruvate and lactate are critical fuel substrates of skeletal muscle particularly during exercise (15, 16, 28). A major source of pyruvate is generated by glycolysis; pyruvate can either serve as a substrate for the mitochondrial TCA cycle to fully catabolize glucose for maximal ATP production, or it can be used for lactate production through a less efficient ATP generation

* This work was supported by Ministry of Science and Technology of China 973 Program Grant 2015CB856300, National Natural Science Foundation of China Grants 31471110 and 81400821, Natural Science Foundation of Jiangsu Province Grant BK20140600 (to Z. G.), and National Institutes of Health Grant RO1DK045416 (to D. P. K.). The authors declare that they have no conflicts of interest with the contents of this article. The content is solely the responsibility of the authors and does not necessarily represent the official views of the National Institutes of Health.

[1] Both authors contributed equally to this work.

[2] To whom correspondence should be addressed: Model Animal Research Center of Nanjing University, 12 Xuefu Rd., Pukou, Nanjing, China 210061. Tel.: 86-25-58641546; Fax: 86-25-58641500; E-mail: ganzj@nju.edu.cn.

[3] The abbreviations used are: PGC, PPARγ coactivator; PPAR, peroxisome proliferator-activated receptor; LDH, lactate dehydrogenase; ERR, estrogen-related receptor; MCK, muscle creatine kinase; WV, white vastus; GC, gastrocnemius; LE, low level of *Ldhb* overexpression; HE, high level of *Ldhb* overexpression; NTG, nontransgenic; RER, respiratory exchange ratio; SDH, succinate dehydrogenase; OCR, oxygen consumption rate; FCCP, carbonyl cyanide *p*-trifluoromethoxyphenylhydrazone; ECAR, extracellular acidification rate; qRT-PCR, quantitative RT-PCR.

pathway. Another significant source of pyruvate is generated by oxidation of lactate, and exercise training is known to increase lactate oxidation in skeletal muscle (29, 30). Lactate dehydrogenase (LDH) is the key enzyme that catalyzes the interconversion of pyruvate and lactate, thereby regulating cellular pyruvate and lactate homeostasis.

LDH functions as a tetrameric complex composed of two distinct isoforms, LDH-A and LDH-B (31–34), encoded by the *Ldha* and *Ldhb* genes, respectively. LDH isoenzyme complexes are classified into LDH1 (B_4), LDH2 (A_1B_3), LDH3 (A_2B_2), LDH4 (A_3B_1), and LDH5 (A_4) based on different combination of LDH-A and LDH-B isoforms (32, 34). The LDH-A isoform is also known as the M isoform, expressed predominantly in skeletal muscle, whereas LDH-B is also referred to H isoform, is expressed primarily in the heart muscle (35). Previously studies have demonstrated that the LDH-A isoenzyme favors the reaction that converts pyruvate to lactate, whereas the LDH-B isoenzyme prefers the reverse reaction that produces pyruvate from lactate (31, 36). We have recently found that *Ldhb* is a glucose oxidation biomarker in skeletal muscle; the expression of *Ldhb* is activated by PPARβ/δ signaling and linked to the high glucose oxidative capacity in MCK-PPARβ/δ muscle (18, 37). In addition, the expression of *Ldhb* was also involved in PGC-1α-mediated control of lactate homeostasis in muscle (38). However, the functional significance of the *Ldhb* in skeletal muscle physiology is unclear.

In this study, we found that *LDHB* expression is induced by exercise in human muscle and negatively correlated with changes in intramuscular pH levels during isometric exercise. We also demonstrated that exercise-induced PGC-1α signaling directly drives the expression of *Ldhb* in skeletal muscle. We speculated that the exercise-induced *Ldhb* contributed to the muscle metabolic adaptations induced by exercise training. Using muscle-specific transgenic mouse lines and primary skeletal myotubes in culture, we found that chronic activation of *Ldhb* in skeletal muscle triggers an adaptive oxidative muscle transformation, leading to increased exercise capacity in MCK-Ldhb transgenic mice. Thus, our results identified a previously unrecognized *Ldhb*-driven alteration in muscle mitochondrial function and suggest a mechanism for the adaptive metabolic response induced by exercise training.

Results

Activation of LDHB Expression by Exercise Is Linked to Muscle Metabolic Parameters in Humans—We have recently shown that LDH-B isoform (*Ldhb*) expression is highly correlated with skeletal muscle glucose oxidation capacity in mice (18, 37). To further explore the physiological relevance of the *LDHB* in humans, muscle samples from trained, active individuals and healthy sedentary controls were analyzed. Previous studies have demonstrated that the active group has higher measures of enhanced exercise performance (including VO_{2max} and ATP_{max}) compared with the sedentary group (19, 39, 40). The characteristics of the human subjects are presented in Table 1. Muscle tissue from the active group exhibited higher *LDHB* gene expression compared with the sedentary control group (Fig. 1*A*). In contrast, the levels of *LDHA* mRNA showed a trend toward a decrease in active muscle (Fig. 1*A*). Additionally, we also examined the expression of *LDHB* in a subgroup of sedentary subjects who underwent an exercise training program. The expression levels of *LDHB* were significantly elevated in human muscle by exercise training (Fig. 1*B*). However, this induction was not observed with *LDHA* mRNA levels (Fig. 1*B*). PGC-1α is a known exercise-induced transcriptional cofactor that regulates expression of many exercise-responsive genes. As shown in Fig. 1*C*, there was a significant positive correlation between *LDHB* and *PGC-1α* mRNA levels in human muscle, suggesting a possible mechanism for exercise-induced *Ldhb* expression. Changes in intramuscular pH levels are a marker of lactate production, because lactate production indicates the generation of a proton that can be measured by the shift in resonance of inorganic phosphate. We also assessed the relationship between *LDHB* expression and changes in intramuscular pH levels during isometric exercise while measuring PCr recovery rate. As shown in Fig. 1*D*, a strong negative correlation was observed between the expression of *LDHB* and changes in intramuscular pH levels. This is consistent with the fact that *Ldhb* is the key enzyme responsible for lactate oxidation and reduction (31, 36). In contrast, *LDHA* expression levels did not exhibit a significant correlation with either PGC-1α levels or changes in intramuscular pH levels (Fig. 1, *C* and *D*). Together, these results demonstrate that *LDHB*, but not *LDHA*, is induced by exercise and linked to muscle metabolic parameters in humans.

TABLE 1
Human subject characteristics
The data represent the means ± S.E. The differences were analyzed using a two-sample *t* test, with a statistically significant difference defined as $p < 0.05$.

	Active ($n = 8$)	Sedentary control ($n = 17$)	*p* value
Age (years)	23.25 ± 1.28	27.63 ± 1.22	0.0358
Weight (kg)	75.48 ± 3.11	80.24 ± 2.52	0.2753
Body-mass index (kg/m^2)	23.52 ± 1.02	25.69 ± 0.64	0.1045
Fat mass (%)	12.62 ± 1.10	22.42 ± 1.22	<0.0001
Fasting glucose (mg/dl)	88.63 ± 2.05	92.35 ± 2.11	0.2838
ATP_{max} (mM/s)	1.01 ± 0.08	0.66 ± 0.03	<0.0001
Type I fiber (%)	52.68 ± 4.71	29.37 ± 2.23	<0.0001
$VO_{2\,max}$ (ml/kg/min)	50.24 ± 1.56	32.41 ± 1.50	<0.0001

Ldhb Expression Is Regulated by Exercise-induced PGC-1α—The observation that *LDHB* gene expression was positively correlated with PGC-1α levels in human muscle led us to explore the link between PGC-1α signaling and the expression of *Ldhb*. Given that *Ldhb* is expressed predominantly in the heart, we first conducted PGC-1 loss of function studies in mouse heart. As shown in Fig. 2*A*, levels of *Ldhb* mRNA were down-regulated in PGC-1α-deficient (PGC-1$\alpha^{-/-}/\beta^{+/+}$) hearts and further reduced in PGC-1α/β deficient (PGC-1$\alpha^{-/-}/\beta^{f/f}$/MCK-Cre) hearts when compared with controls (PGC-1$\alpha/\beta^{+/+}$). In contrast, *Ldha* mRNA levels were not changed in PGC-1α/β-deficient heart. Consistent with these results in the heart, disruption of PGC-1α (PGC-1α KO) in skeletal muscle resulted in diminished expression of *Ldhb*, but not *Ldha* (Fig. 2*B*). These data suggest that PGC-1α and PGC-1β function redundantly *in vivo* to regulate the expression of *Ldhb* gene. We also conducted PGC-1α gain of function in primary skeletal myotubes, in which the basal expression of *Ldhb* is low. Consistent with previously report (38), there was an increase in *Ldhb* mRNA, but not *Ldha* mRNA levels, in skeletal myotubes subjected to ade-

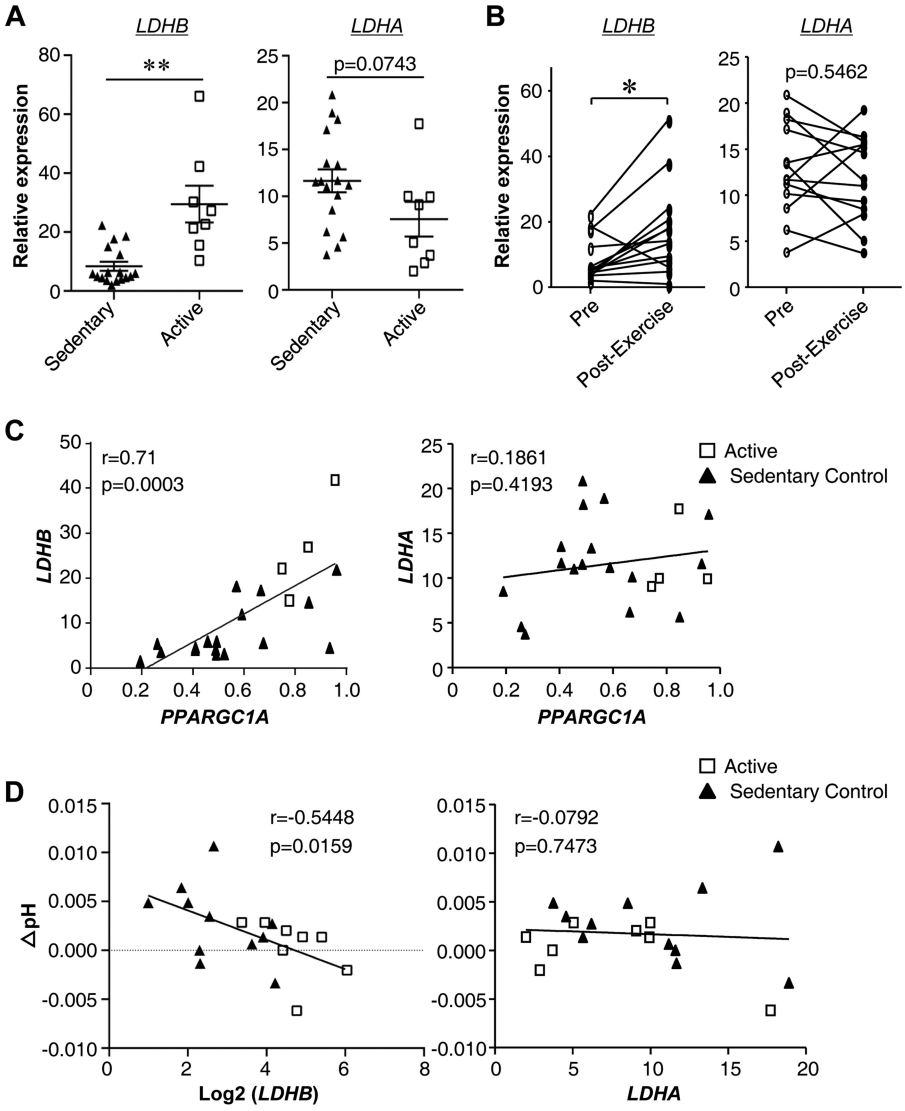

FIGURE 1. **LDHB expression is induced by exercise in human muscle and negatively correlated with changes in intramuscular pH levels during muscle contraction.** Samples from 4–8 active and 15–17 healthy sedentary controls were used for this analysis. mRNA expression levels of *LDHB*, *LDHA*, and *PPARGC1A* was determined by qRT-PCR. The data represent the means ± S.E. *A*, *LDHB* and *LDHA* expression in sedentary and active human muscle analyzed using a two-sample *t* test ($n = 8–17$). **, $p < 0.01$ *versus* sedentary controls. *B*, skeletal muscle *LDHB* and *LDHA* expression pre- and postexercise training of lean sedentary subjects. The differences were analyzed using paired Student's *t* test ($n = 13$). *, $p < 0.05$. *C*, Spearman correlation between *LDHB* and *LDHA* gene expression and *PPARGC1A*. *D*, Pearson correlation between *LDHB* and *LDHA* gene expression and ΔpH (changes in pH levels).

novirus-mediated overexpression of PGC-1α (Ad-PGC-1α) compared with a control vector (Ad-GFP) (Fig. 2*C*). The expected LDH isoenzyme activity shifts were confirmed by activity gel studies (Fig. 2*D*). We have recently shown a functional MEF2 site in the *Ldhb* promoter (18). Although a PGC-1α-responsive ERR site has also been described in the *Ldhb* promoter recently (38), we next sought to determine the precise mechanism whereby PGC-1α induces *Ldhb* gene transcription. Approximately 1.8 kb of the m*Ldhb* gene promoter region containing the MEF2 and −149 ERR-RE binding sites was cloned into a PGL3 reporter vector (m*Ldhb*.Luc.1791). Cotransfection of m*Ldhb*.Luc.1791 with PGC-1α in C2C12 myotubes resulted in robust activation of the promoter (Fig. 2*E*). To map the *cis*-acting region conferring the PGC-1α activation, cotransfection experiments were conducted with reporter constructs containing two serial deletions of the m*Ldhb* promoter (Fig. 2*F*). Both the basal and PGC-1α induced promoter activity decreased upon deletion of the promoter regions from −1791 to −869 bp containing the MEF2 sites, suggesting a role of the MEF2 site in the maximal induction of *Ldhb* promoter by PGC-1α. The basal promoter activity continues to decrease upon deletion the regions from −869 to −122 bp containing the previously identified −149 ERR-RE. Surprisingly, PGC-1α-mediated activation was maintained upon deletion of the −149 ERR-RE, suggesting the existence of an additional *cis*-regulatory element in the proximal promoter region. The analysis of the DNA sequence of *Ldhb* proximal promoter region identified two additional conserved putative ERR-binding sites around the previously identified −149 ERR-RE (Fig. 2*G*). The two new ERR sites were excellent match for an ERR-binding site (Fig. 2*G*). To evaluate the functionality of the newly identified ERR binding sites for PGC-1α coactivation, promoter mutational studies were next performed. Mutation of the two putative ERR response element significantly attenuated the activation of

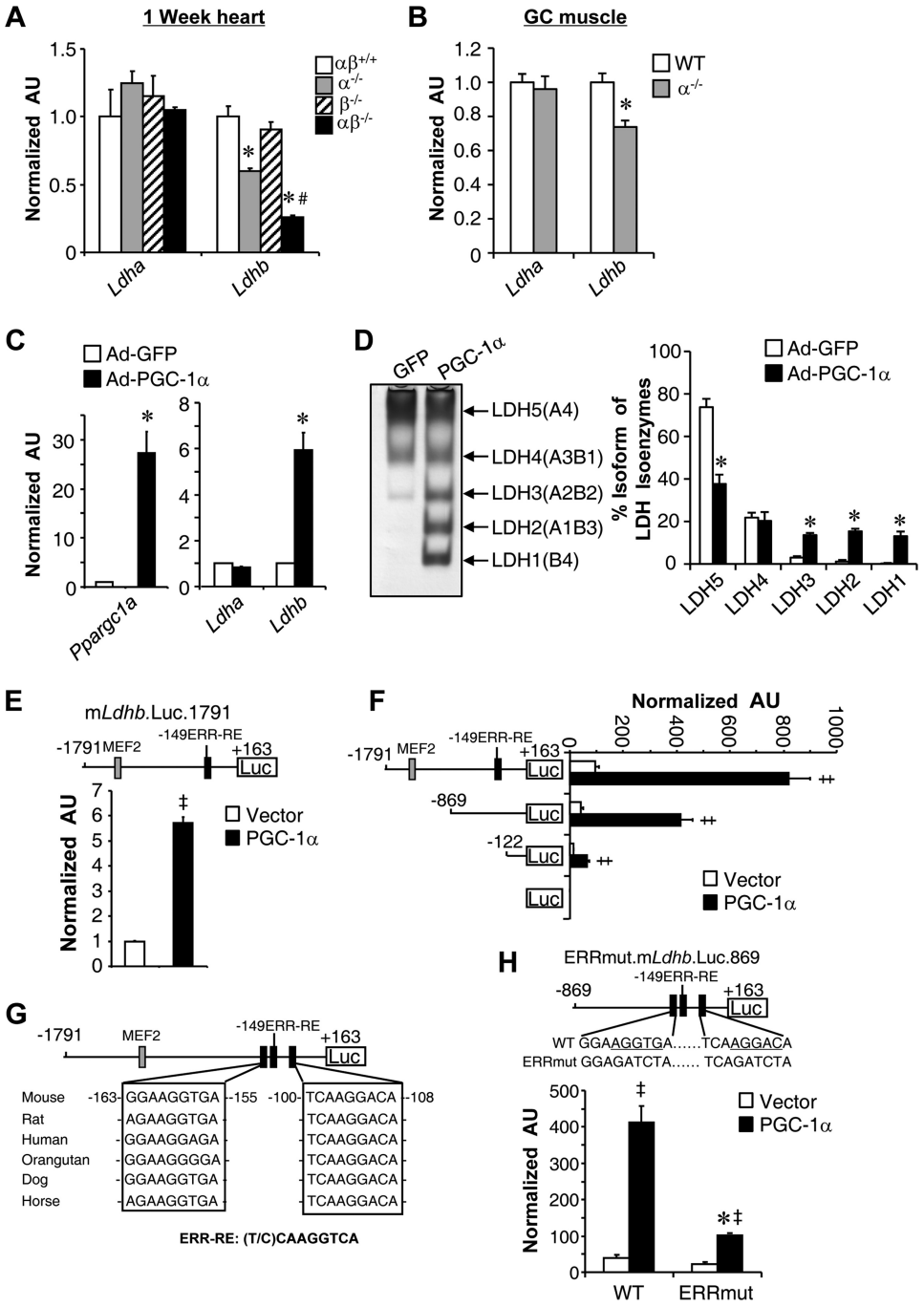

FIGURE 2. **Ldhb expression is regulated by exercise-induced PGC-1α.** *A*, expression of the *Ldhb* and *Ldha* genes (qRT-PCR) in the hearts of PGC-1$\alpha^{-/-}\beta^{f/f/MCK\text{-}Cre}$ mice ($n = 4$–7 mice/group). *B*, expression of the *Ldhb* and *Ldha* genes (qRT-PCR) in the GC muscle of PGC-1α KO mice ($n = 10$–12 mice/group). *C*, *Ldhb*, *Ldha*, and *Ppargc1a* transcript levels in myotubes harvested from muscle of WT mice and subjected to Ad-PGC-1α overexpression compared with GFP control ($n = 3$). *D*, *left panel*, LDH isoenzymes were separated by polyacrylamide gel electrophoresis using whole cell extracts from WT myotubes subjected to Ad-PGC-1α overexpression. A representative gel is shown. *Right panel*, quantification of LDH isoenzyme activity gel electrophoresis. The values represent the mean percentages (± S.E.) of total LDH activity ($n = 3$). *E*, the m*Ldhb*.Luc.1791 promoter reporter was used in cotransfection studies in C2C12 myotubes in the presence or absence of PGC-1α ($n = 3$). *F*, results of transient transfection performed with mouse *Ldhb* reporter m*Ldhb*.Luc.1791 and truncation mutants of m*Ldhb*.Luc.859 or 122 in C2C12 myotubes in the presence or absence of PGC-1α ($n = 3$). *G*, schematic shows the putative conserved MEF2 and ERR binding sites within the *Ldhb* promoter regions. *H*, *top panel*, site-directed mutagenesis was used to abolish the ERR response elements. *Bottom panel*, the m*Ldhb*.Luc.859 (WT) or ERRmut.m*Ldhb*.Luc.859 promoter reporters was used in cotransfection studies in C2C12 myotubes in the presence or absence of PGC-1α ($n = 3$). *, $p <$ 0.05 *versus* corresponding controls; #, $p < 0.05$ *versus* $\alpha^{-/-}$; ‡, $p < 0.05$ *versus* vector alone. All values represent the means ± S.E.

m*Ldhb*.Luc.869 by PGC-1α (Fig. 2*H*). Together, these results demonstrate that multiple *cis*-regulatory elements, including the distal MEF2 and proximal ERR binding sites in the Ldhb promoter, contribute to the full activation of the *Ldhb* gene by PGC-1α.

Activation of Ldhb Leads to Reciprocal Reduction in Ldha Level in Skeletal Muscle—We next determined whether forced activation of *Ldhb* in skeletal muscle is able to affect muscle function. As an initial step, we examined the expression patterns of *Ldhb* in different muscle types from adult wild type

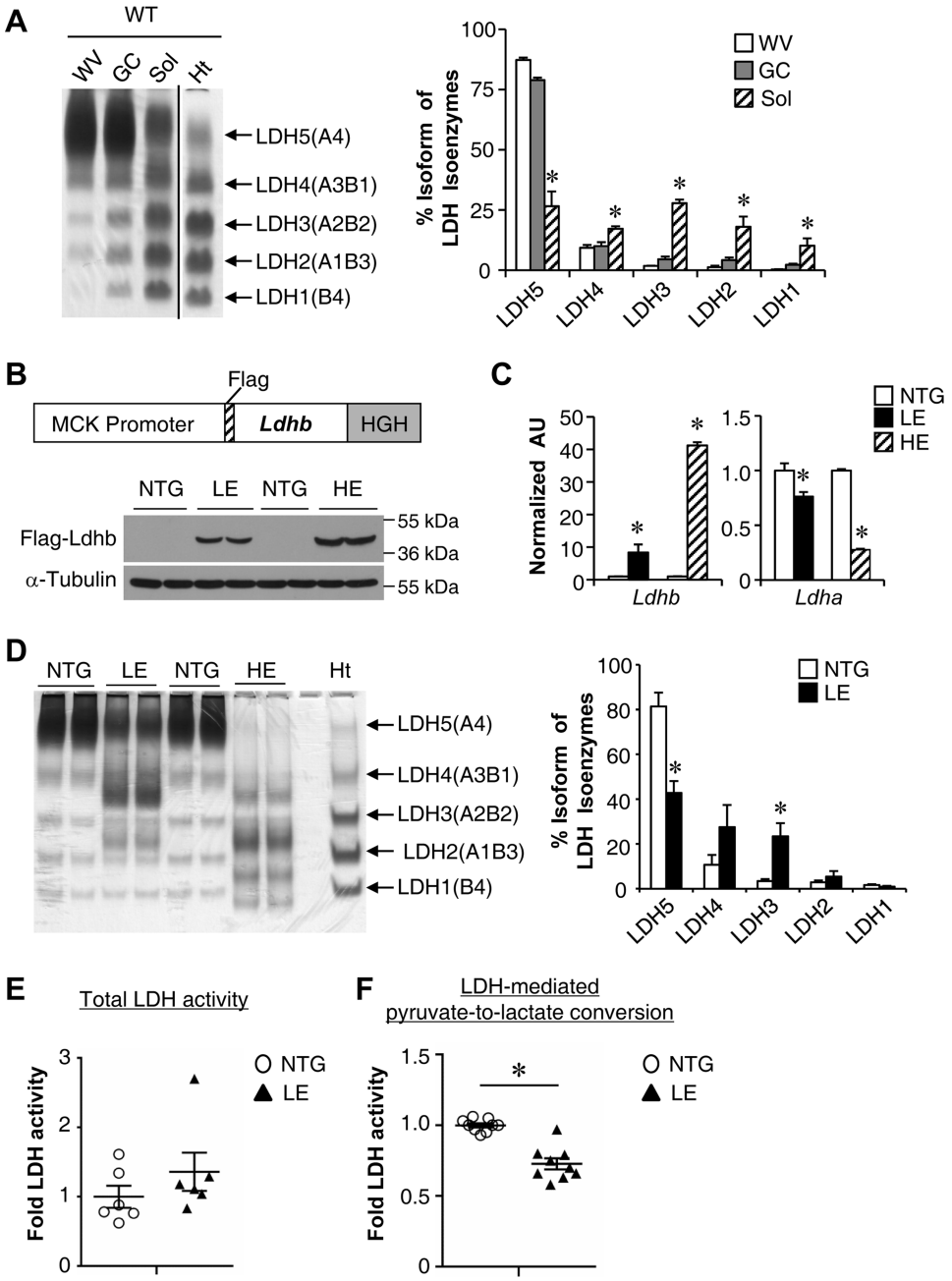

FIGURE 3. **Ldhb overexpression in skeletal muscle.** *A*, *left panel*, a representative LDH isoenzyme activity gel is shown. Isoenzymes were separated by polyacrylamide gel electrophoresis using whole cell extracts from WV, GC, soleus (*Sol*), and heart (*Ht*) muscle from WT mice. Note a distinct shift toward the Ldhb-containing isoenzymes LDH4, LDH3, LDH2, and LDH1 with a concomitant reduction in LDH5 (which lacks the Ldhb isoenzyme) in the soleus. *Right panel*, quantification of LDH isoenzyme activity gel electrophoresis ($n = 3$ mice). *B*, *top panel*, the schematic depicts the MCK-Ldhb construct used for transgene production. *Bottom panel*, representative Western blotting analysis performed with GC muscle total protein extracts prepared from NTG mice and two lines of MCK-Ldhb (LE and HE) mice using FLAG and α-tubulin (control) antibodies. *C*, expression of the *Ldhb* and *Ldha* genes (qRT-PCR) in the GC muscle from the indicated genotypes ($n = 4–6$ mice/group). *D*, *left panel*, a representative LDH isoenzyme activity gel using whole cell extracts from GC muscle from the indicated genotypes. *Right panel*, quantification of LDH isoenzyme activity gel electrophoresis ($n = 6$ mice/group). *E*, total LDH enzymatic activity in WV muscle of MCK-Ldhb (LE) mice ($n = 6$ mice/group). *F*, enzymatic activity of LDH-mediated pyruvate to lactate conversion in WV muscle of MCK-Ldhb (LE) mice ($n = 9$ mice/group). *, $p < 0.05$ *versus* corresponding controls. All values represent the means ± S.E.

mice. Consistent with the PGC-1α regulatory circuit controlling *Ldhb* expression, *Ldhb* was expressed much higher in slow fiber-dominant soleus muscle compared with fast fiber-enriched white vastus (WV) and gastrocnemius (GC) muscle (Fig. 3*A*). The muscle creatine kinase promoter was next used to generate skeletal muscle-specific *Ldhb* transgenic mice (MCK-Ldhb mice). Two independent lines of MCK-Ldhb mice with low (LE) and high (HE) levels of *Ldhb* overexpression were generated and characterized (Fig. 3, *B* and *C*). The MCK-Ldhb transgene transcript was expressed in a skeletal muscle-specific manner, and we observed no change in *Ldhb* expression in the heart (data not shown). Interestingly, real time quantitative PCR demonstrated that activation of *Ldhb* in skeletal muscle leads to a reciprocal suppression of the *Ldha* mRNA level (Fig. 3*C*). LDH isoenzyme assay using lactate as a substrate displayed a pronounced shift toward an *Ldhb*-containing isoenzyme

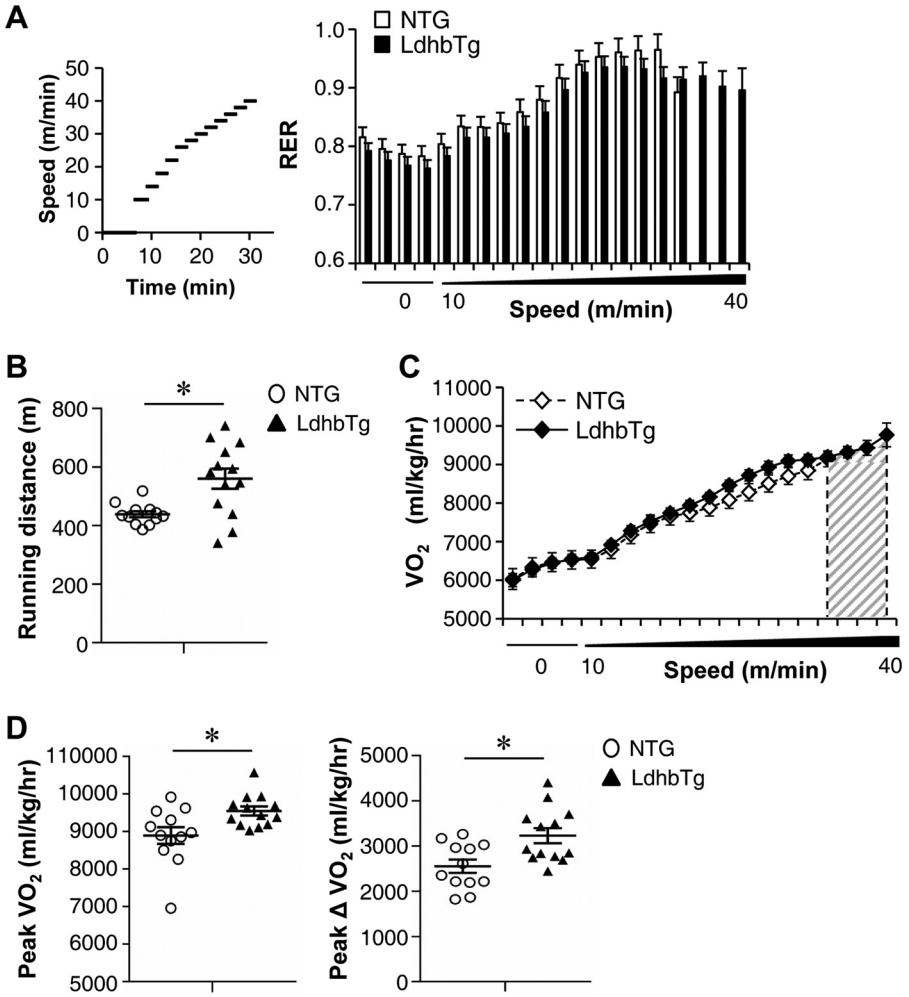

FIGURE 4. **MCK-Ldhb mice exhibit increased exercise performance and enhanced oxygen consumption during exercise.** *A*, *left panel*, schematic depicts the increments of speed over time. *Right panel*, RER during a graded exercise regimen as described under "Experimental Procedures" ($n = 12–13$ mice/group). Notably, MCK-Ldhb (LE) female mice were able to exercise at a higher speed before exhaustion. *B*, the scatter plots represent the mean running distance (± S.E.) in *A*. *C*, VO_2 (oxygen consumption) during an exercise bout in female MCK-Ldhb (LE) and NTG mice ($n = 12–13$ mice/group). The *gray-hatched area* in the VO_2 line graphs illustrate the difference in speed to exhaustion in MCK-Ldhb (LE) mice compared with NTG controls. *D*, peak VO_2 (VO_2 at the time of failure) and peak ΔVO_2 (increase in oxygen consumption) are graphed. The values represent means ± S.E. ($n = 12–13$ mice/group). *, $p < 0.05$ *versus* NTG.

complex in MCK-Ldhb (LE and HE) muscle (Fig. 3*D*). Notably, the reciprocal regulation of *Ldhb* and *Ldha* was much greater in MCK-Ldhb (HE) compared with MCK-Ldhb (LE) (Fig. 3*D*), suggesting a mechanism whereby *Ldhb* autoregulates the composition of the LDH isoenzyme complex. We subsequently focused on the MCK-Ldhb (LE) line, because of relative physiological overexpressing of *Ldhb*. A series of studies were next conducted to determine the effect of *Ldhb* overexpression on muscle LDH enzymatic activity. Whereas the total LDH activity showed an increase trend in MCK-Ldhb (LE) muscle, the enzymatic activity of LDH-mediated pyruvate to lactate conversion was significantly reduced in skeletal muscle of MCK-Ldhb (LE) compared with NTG controls (Fig. 3, *E* and *F*). These results are consistent with *Ldhb* catalyzing the production of lactate from pyruvate slower and less efficiently relative to *Ldha*, thus diverting pyruvate into mitochondria for complete oxidation (32).

MCK-Ldhb Mice Exhibit Increased Exercise Performance and Enhanced Oxygen Consumption during Exercise—MCK-Ldhb (LE) mice appeared normal on inspection and did not exhibit an overt metabolic phenotype compared with NTG littermates on standard chow. This includes similar body weight, food intake, energy expenditure, and fasting glucose levels (data not shown). To assess the physiological effects of chronic increased *Ldhb* expression in skeletal muscle, exercise stress testing was conducted in MCK-Ldhb mice. The real time respiratory exchange ratio (RER) was measured during a run to exhaustion exercise protocol. Consistent with a switch to carbohydrates as the chief fuel during exercise, the RER increased with exercise in both MCK-Ldhb and in the NTG control group (Fig. 4*A*). Despite no change in RER levels during exercise, the MCK-Ldhb (LE) mice exercised significantly longer distance compared with the control group (Fig. 4, *A* and *B*). In addition, the MCK-Ldhb (LE) mice consumed more oxygen during the exercise period (as reflected by an increase in peak VO_2) (Fig. 4, *C* and *D*). It has been shown that whole body oxygen utilization during exercise (peak ΔVO_2) largely reflects changes occurring within the exercising muscle (41). Peak ΔVO_2 was significantly higher in the MCK-Ldhb (LE) mice compared with NTG controls (Fig. 4*D*). These results demonstrate that chronic increased *Ldhb* expression in skeletal muscle is able to affect muscle performance.

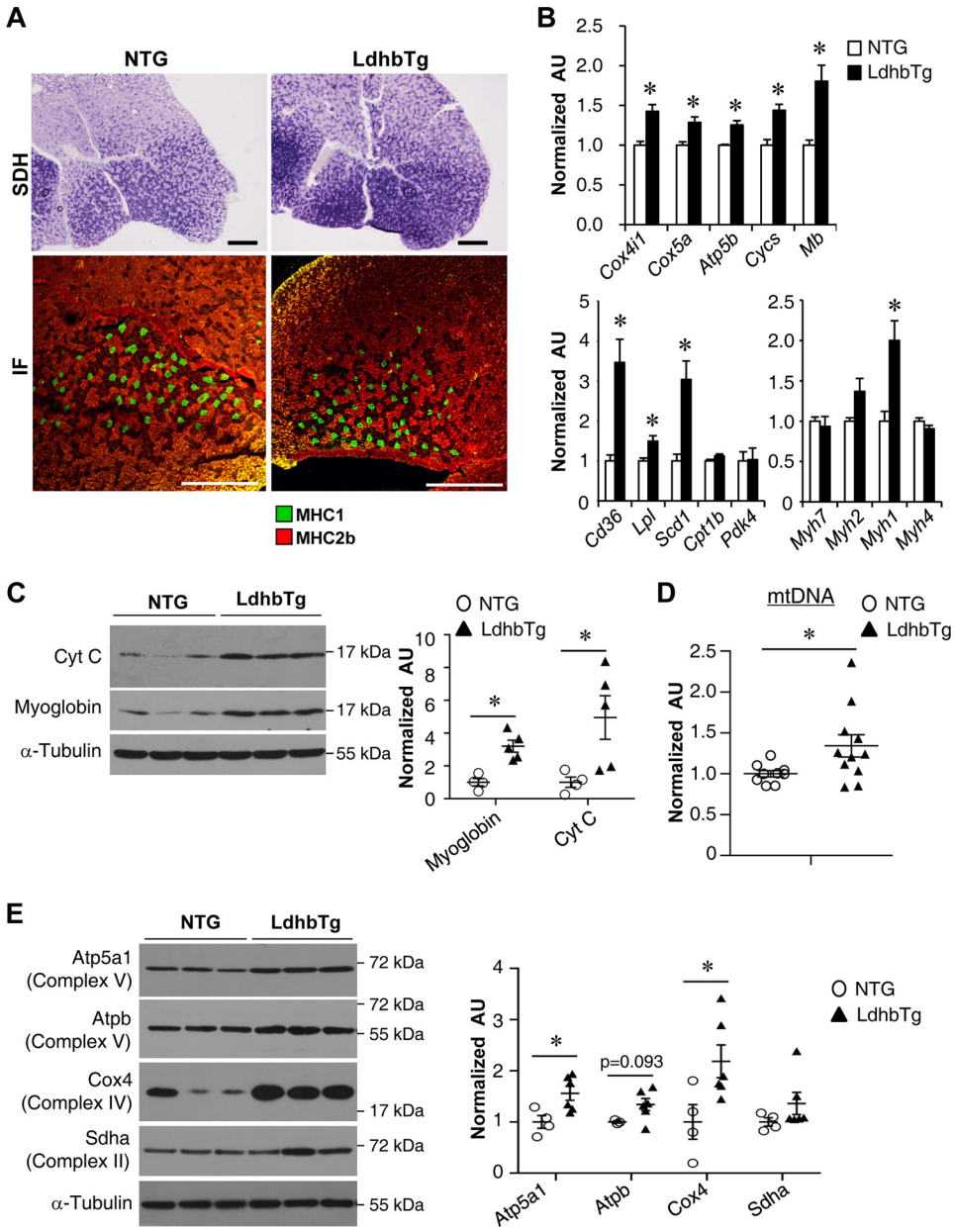

FIGURE 5. **MCK-Ldhb muscle is reprogrammed for increased capacity for mitochondrial oxidation.** *A*, *top row*, cross-section of the GC muscle from a 3-month-old female NTG and MCK-Ldhb (LE) stained for SDH. *Bottom row*, representative MHC immunofluorescence (*IF*) in the GC muscles of the indicated genotypes. *Green*, MHC1; *red*, MHC2b ($n = 3–8$ mice/group). *Scale bars*, 500 μm. *B*, expression of genes involved in mitochondrial oxidation, fuel metabolism, and contractile myosin isoforms (qRT-PCR) in GC muscle from the NTG and MCK-Ldhb (LE) mice ($n = 4–6$ mice/group). *C*, *left panel*, representative Western blotting analysis performed with WV muscle total protein extracts prepared from the NTG and MCK-Ldhb (LE) mice using cytochrome *c*, myoglobin, and α-tubulin (control) antibodies. *Right panel*, quantification of the myoglobin/tubulin and cytochrome *c*/tubulin signal ratios normalized (= 1.0) to the NTG control ($n = 4–5$ mice/group). *D*, results of qPCR to determine mitochondrial DNA levels in GC muscle of the MCK-Ldhb (LE) mice ($n = 9–11$ mice/group). *E*, *left panel*, representative Western blotting analysis performed with WV muscle total protein extracts prepared from the NTG and MCK-Ldhb (LE) mice using Atp5a1, Atpb, Cox4, Sdha, and α-tubulin (control) antibodies. *Right panel*, quantification of the Western blot shown in the *left panel*. Atp5a1/tubulin, Atpb/tubulin, Cox4/tubulin, and Sdha/tubulin signal ratios were normalized (1.0) to the NTG control ($n = 3–6$ mice/group). *, $p < 0.05$ *versus* NTG. All values represent the means ± S.E.

MCK-Ldhb Muscle Is Reprogrammed for Increased Capacity for Mitochondrial Oxidation—The increase in exercise capacity and oxygen consumption in MCK-Ldhb mice led us to investigate the potential impact of activating *Ldhb* on muscle oxidative mitochondrial activity. We first performed histochemical staining for succinate dehydrogenase (SDH), a hallmark for oxidative metabolism in skeletal muscle (42). Interestingly, the SDH enzymatic activity was higher in the GC muscle of MCK-Ldhb mice compared with their NTG littermate controls (Fig. 5*A*), suggesting that chronic activation of *Ldhb* triggers an adaptive muscle oxidative reprograming. Interestingly, however, no change in MHC1 immunofluorescence was observed in the GC muscle of MCK-Ldhb mice compared with their NTG controls (Fig. 5*A*). To further evaluate the effect of *Ldhb* in regulating mitochondrial oxidative capacity, we conducted comparative analysis of RNA isolated from GC muscle of the MCK-Ldhb mice and NTG littermate controls. Real time PCR revealed that the expression of mitochondrial oxidation genes

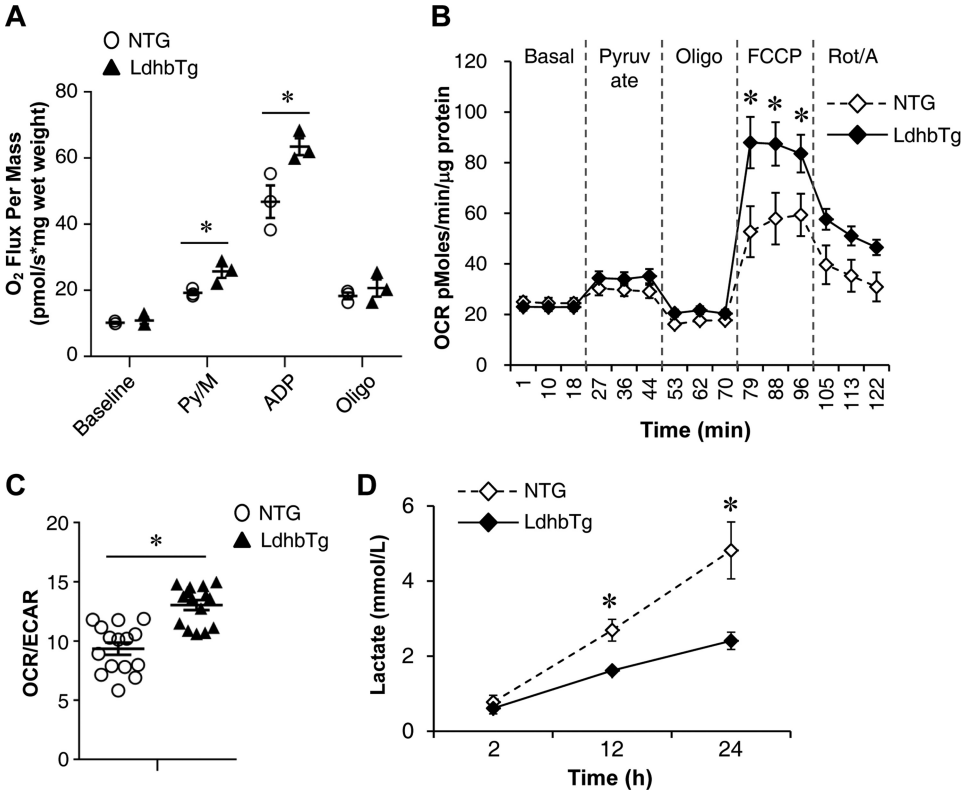

FIGURE 6. **Increased mitochondrial function in MCK-Ldhb skeletal muscle.** *A*, mitochondrial respiration rates were determined from the extensor digital longus muscle of the indicated genotypes using pyruvate/malate as substrate. Pyruvate/malate (*Py/M*)-stimulated, ADP-dependent respiration, oligomycin-induced (*Oligo*), and the respiratory control ratio are shown ($n = 3$ mice/group). *B*, OCRs in primary mouse myotubes isolated from the NTG and MCK-Ldhb (LE) mice. Basal OCR was first measured, followed by administration of 10 mM sodium pyruvate, 2 μM oligomycin (to inhibit ATP synthase), uncoupler FCCP (2 μM), or rotenone/antimycin (*Rot/A*) (1 μM) as indicted. *C*, OCR/ECAR ratio using pyruvate as substrate indicates a shift in cellular energy production to oxidative phosphorylation ($n = 3$ separate experiments done with 5 biological replicates). *D*, lactate concentrations in culture medium from primary mouse myotubes isolated from the NTG and MCK-Ldhb (LE) mice ($n = 3$). *, $p < 0.05$ *versus* NTG controls. All values represent the means ± S.E.

(*Cox4i1*, *Cox5a*, *Atp5b*, *Cycs*, and *Mb*) was induced in the GC muscle of MCK-Ldhb mice compared with NTG controls (Fig. 5*B*). Moreover, we also found an increased expression of biomarker genes associated with fatty acid metabolism (*Cd36*, *Lpl*, and *Scd1*) in MCK-Ldhb muscle (Fig. 5*B*). Consistent with the fiber typing results, there was no difference in the expression of *Myh7*, which encodes the myosin heavy chain for type I fibers in MCK-Ldhb muscle (Fig. 5*B*), although the expression of the oxidative type IIx myosin gene *Myh1* was increased in MCK-Ldhb muscle (Fig. 5*B*). The oxidative transformations in MCK-Ldhb muscle were also validated at the protein level, because the expression of the oxidative biomarkers myoglobin and cytochrome *c* was induced in MCK-Ldhb WV muscles compared with NTG controls (Fig. 5*C*). The mitochondrial DNA levels were increased in MCK-Ldhb GC muscle compared with NTG controls (Fig. 5*D*). In addition, Western blotting revealed significant increases in several components of the electron transport chain (*e.g.* Atp5a1 and Cox4) in MCK-Ldhb WV muscle (Fig. 5*E*). Together, these results demonstrate that chronic activation of *Ldhb* reprograms muscle for increased mitochondrial oxidative capacity.

Increased Mitochondrial Function in MCK-Ldhb Skeletal Muscle—Mitochondrial respiration rates were determined in the extensor digital longus muscle of the MCK-Ldhb (LE) mice and corresponding NTG controls. Consistent with the oxidative transformations in MCK-Ldhb muscle, pyruvate-driven state 3 respiration rates were significantly higher in MCK-Ldhb muscle compared with the NTG controls (Fig. 6*A*). To directly determine the effects of activating *Ldhb* on muscle mitochondrial function, oxygen consumption rates (OCRs) were also measured in primary myotubes isolated from MCK-Ldhb skeletal muscle. As shown in Fig. 6*B*, activation of *Ldhb* significantly stimulated the OCR in the presence of the uncoupler FCCP, a sign of enhanced mitochondrial function. We also determined the extracellular acidification rate (ECAR) (a measure of glycolysis) along with OCRs in these cells. *Ldhb* overexpression significantly induced OCR/ECAR ratio, indicative of a shift toward more oxidative phosphorylation for cellular energy production (Fig. 6*C*). Consistent with the aerobic metabolism in MCK-Ldhb myotubes, the rate of lactate production decreased in myotubes isolated from MCK-Ldhb muscle compared with NTG controls (Fig. 6*D*). These results demonstrate that chronic activation of *Ldhb* in muscle cells promotes a shift toward a more oxidative phenotype, which is consistent with the phenotypic changes observed in MCK-Ldhb mice.

Discussion

Mitochondrial oxidative metabolism and energy production are critical for muscle performance. Exercise is known to be the best medicine for many chronic illnesses including obesity, diabetes, muscular diseases, and aging, by promoting favorable metabolic and structural adaptations to improve muscle fitness

(6–13). Delineation of the molecular regulatory pathways involved in the beneficial effects of exercise training on muscle fuel metabolism has implications for new therapeutic approaches for many human diseases associated with muscle bioenergetics defects. Herein, we discover a novel mechanism for exercise-induced metabolic changes in skeletal muscle. Our results support the following conclusions: 1) *LDHB* expression is induced by exercise in human muscle and negatively correlated with changes in intramuscular pH levels during muscle contraction; 2) exercise-induced PGC-1α signaling directly regulates the transcription of the *Ldhb* gene by coactivating multiple *cis*-regulatory elements in the *Ldhb* promoter; and 3) chronic activation of *Ldhb* triggers a secondary mitochondrial oxidative metabolism program in skeletal muscle. We therefore identify a previously unrecognized *Ldhb*-driven alteration in muscle mitochondrial function and suggest a mechanism for the adaptive metabolic response induced by exercise training.

Previous studies have established that the PGC-1α transcriptional regulatory circuit, including nuclear receptors PPAR and ERR, is a key transducer of skeletal muscle adaptation to exercise by directly regulates the expression of genes involved in mitochondrial fuel metabolism (17–25). We have recently shown that *Ldhb* is a downstream target of PPARβ/δ signaling (18, 37). In addition, the PGC-1α-ERR axis has also been implicated in the regulation of *Ldhb* expression (38). In the present study, our data suggest that *Ldhb* is a regulator of mitochondrial function that acts downstream of the PGC-1α/nuclear receptor regulatory circuit. Exercise training induces the expression of both PGC-1α and *Ldhb* in muscle. It is likely that the *Ldhb*-driven alteration of skeletal muscle mitochondrial function contributes the broad effect of exercise PGC-1α signaling on muscle metabolic adaptations.

The observed role of *Ldhb* in regulating muscle mitochondrial function was surprising, given that *Ldhb* is a glycolytic enzyme responsible for lactate oxidation and reduction (31, 36). Several lines of evidence presented here support the conclusion that chronic activation of *Ldhb* triggers a secondary beneficial muscle metabolic reprograming, in addition to regulating pyruvate/lactate homeostasis. First, MCK-Ldhb mice are able to run longer during exercise. Second, diverse aspects of aerobic metabolism, including the capacity for oxygen consumption during exercise, muscle SDH activity, and mitochondrial respiration, are increased in MCK-Ldhb muscle compared with NTG controls. Third, a broad array of mitochondrial metabolism genes and oxidative biomarkers are induced in MCK-Ldhb muscle compared with NTG controls.

Whereas our results provide significant evidence that increased *Ldhb* activity affects muscle mitochondrial function, the molecular basis of this finding was not fully delineated in this study. Interestingly, we do not see significant changes in oxidative biomarkers in younger MCK-Ldhb muscle (6 weeks old) compared with NTG controls. This could relate to the age difference. Alternatively, the secondary mitochondrial gene programs triggered by chronic activation of *Ldhb* are not manifest as early in 6-week-old muscle because other postnatal programs are dominant during the first several weeks after birth (42). *Ldhb* has recently been shown to locate outside of the mitochondrial matrix (43), and lactate oxidation was shown to regulate mitochondrial oxidative gene expression in muscle cells (44). It is possible that an alteration in pyruvate/lactate oxidation in MCK-Ldhb muscle triggers the mitochondrial oxidative gene expression. It is also intriguing to speculate that *Ldhb* can serve as a unique glycolytic enzyme that could directly affect muscle metabolic gene expression. Consistent with this later notion, the glycolytic enzyme complex SASEME has recently been shown to sense glucose metabolism and directly regulate chromatin modifications (45). Whether such mechanisms are relevant to our study remains to be determined; future studies aimed at assessing the mechanism whereby muscle metabolic reprograming is altered in MCK-Ldhb muscle will likely require metabolic profiling and genome-wide chromatin survey.

We found that the LDH isoenzyme complex was dynamically regulated in human and mouse skeletal muscle. The induced *LDHB* expression during exercise is consistent with previous reports that exercise training increases lactate oxidation in human muscle (29, 30, 46, 47). Our data suggest there were both PGC-1α-dependent and independent mechanisms that regulate the LDH isoenzyme composition. First, our study reveals an intriguing autoregulatory loop whereby *Ldhb* directly controls LDH isoenzyme complex, given that activation of *Ldhb* leads to reciprocal reduction in *Ldha* level in skeletal muscle. Second, our data also demonstrated that *Ldhb* expression is regulated by exercise-induced PGC-1α, providing a mechanism for exercise-induced *Ldhb* expression. Although a PGC-1α-responsive ERR binding site (-149 ERR-RE) has been previously described (38), the functionality of the *Ldhb* gene promoter has not been fully characterized. Using a robust *Ldhb* promoter reporter assay in C2C12 myotubes, we were able to identify two additional functional ERR-REs in the *Ldhb* promoter. In addition, consistent with our previous report (18), our data also support the involvement of the distal MEF2 site for both the basal and full activation of the *Ldhb* promoter by PGC-1α. The involvement of the MEF2 site is also corroborated by the fact that slow oxidative muscle fibers with higher MEF2 activity are enriched in *Ldhb*, whereas the fast glycolytic muscle fibers have the opposite effect.

In summary, we have identified exercise-induced *Ldhb* as a novel regulator of mitochondrial oxidative metabolism in skeletal muscle. Future studies aimed at the mechanisms involved in triggering the adaptive responses could yield new therapeutic targets aimed at the prevention or treatment of diseases associated with muscle bioenergetics defects.

Experimental Procedures

Animal Studies—All animal studies were conducted in strict accordance with the institutional guidelines for the humane treatment of animals and were approved by the institutional animal care and use committees at the Model Animal Research Center of Nanjing University.

Generation of MCK-Ldhb Mice—To generate mice with muscle-specific *Ldhb* overexpression, a cDNA encoding the mouse *Ldhb* gene was cloned into the EcoRV site downstream of the mouse MCK gene promoter (kind gift of E. N. Olson, University of Texas Southwestern). The transgene was linearized with XhoI and SacII digestion and microinjected into

C57BL/6J embryos by the transgenic mouse facility at the Model Animal Research Center of Nanjing University. Transgenic mice were identified by PCR amplification of a 722-bp product using primers specific for *Ldhb* (5′-CAGACAATGACAGTGAGAACTGGAAGGAGG) and the human growth hormone poly(A) component of the MCK construct (5′-ATTGCAGTGAGCCAAGATTGTGCCACTGCA). Two independent lines were generated, exhibiting low and high levels of transgenic expression (LE and HE). Unless specifically indicated, the results described here were generated using the low expressing MCK-Ldhb line (LE), compared with corresponding NTG controls. Of note, the majority of the phenotypic characterization of these mice was performed in female MCK-Ldhb mice. In addition, several readouts, including oxidative biomarkers, were similarly induced in male MCK-Ldhb mice. The PGC-1α/βf/f/MCK-Cre mice have been described previously (48).

Human Studies—After signing the informed written consent approved by the Pennington Biomedical Research Center ethical review board, patients were enrolled in clinical trial performed at the Pennington Biomedical Research Center (Baton Rouge, LA). Volunteers qualified for the study (ACTIV; Clinicaltrials.gov ID NCT00401791) if they ranged in age from 20 to 40, had a body-mass index of 20–30 kg/m^2, were non-diabetic, were taking no medications, and were otherwise healthy. After baseline testing, 13 nonobese sedentary subjects participated in an exercise training protocol consisting of alternating day sessions of a progressive 30–60-min interval protocol (75–85% maximum aerobic capacity ($VO_{2\,max}$)) and a 50-min aerobic protocol (70% $VO_{2\,max}$), both performed on a stationary bicycle. Subjects exercised on 13 days of a 3-week period. Details on subject characteristics and procedures have been described previously (19, 39, 40). Briefly, after an overnight fast and local anesthesia, skeletal muscle was collected from the vastus lateralis muscle, cleaned, and mounted for fiber typing or flash frozen in liquid nitrogen for RNA isolation.

Mouse Studies—Mice were acclimated (run for 9 min at 10 m/min followed by 1 min at 20 m/min) to the treadmill for 2 consecutive days prior to the experimental protocol. RERs during exercise were determined as described previously (18). Briefly, mice were placed in an enclosed treadmill attached to the Comprehensive Laboratory Animal Monitoring System (Columbus Instruments) for 15 min at a 0° incline and 0 m/min. The mice were then challenged with 2-min intervals of increasing speed at a 0° incline. The increasing speeds used in the protocol were 10, 14, 18, 22, 26, 28, 30, 32, 34, 36, 38, and 40 m/min. The protocol was performed until exhaustion; running distance was derived by calculating the treadmill speed and running time. The measurements were collected before the exercise challenge and throughout the challenge, and peak VO_2 was measured at the time of failure.

Mitochondrial Respiration Studies—Mitochondrial respiration rates were measured in saponin-permeabilized extensor digital longus muscle fibers with pyruvate/malate as substrate as described previously (37). In brief, the muscle fibers were separated and transferred to BIOPS buffer. The muscle fibers bundles were then permeabilized with 50 μg/ml saponin in BIOPS solution. Measurement of oxygen consumption in permeabilized muscle fibers was performed in buffer Z at 37 °C and in the respiration chambers of an Oxygraph 2K (Oroboros Inc., Innsbruck, Austria). Following measurement of basal, pyruvate (10 mM)/malate (5 mM) respiration, maximal (ADP-stimulated) respiration was determined by exposing the mitochondria to 4 mM ADP. Uncoupled respiration was evaluated following addition of oligomycin (1 μg/ml). Respiration rates were determined and normalized to fiber bundle wet weight using Datlab 5 software (Oroboros Inc.), and the data are expressed as pmol O_2 s^{-1} mg wet weight^{-1}.

Histologic Analyses—Muscle tissue was frozen in isopentane that had been cooled in liquid nitrogen. SDH and immunofluorescence staining was performed as previously described (24).

RNA Analyses—Quantitative RT-PCR was performed as described previously, with modifications (18, 19). Briefly, total RNA was extracted from mouse muscle or primary myotubes using RNAiso Plus (Takara Bio). The purified RNA samples were then reverse transcribed using the PrimeScript RT reagent kit with gDNA Eraser (Takara Bio). Real time quantitative RT-PCR was performed using the ABI Prism Step-One system with SYBR® Premix Ex Taq™ (Takara Bio). Specific oligonucleotide primers for target gene sequences are listed below. Arbitrary units of target mRNA were corrected to the expression of *36b4*. For mouse gene, the following primers were used: *36b4*, 5′-ATCCCTGACGCACCGCCGTGA, 5′-TGCATCTGCTTGGAGCCCACGT; *Cox4i1*, 5′-TACTTCGGTGTGCCTTCGA, 5′-TGACATGGGCCACATCAG; *Cox5a*, 5′-TTAAATGAATTGGGAATCTCCAC, 5′-GTCCTTAGGAAGCCCATCG; *Atp5b*, 5′-GCAGGGACAGCAGACTGG, 5′-GCCATCCATAGCAATAGTTCTGA; *Scd1*, 5′-TTCCCTCCTGCAAGCTCTAC, 5′-CAGAGCGCTGGTCATGTAGT; *Cpt1b*, 5′-GAGTGACTGGTGGGAAGAATATG, 5′-GCTGCTTGCACATTTGTGTT; *Mb*, 5′-CCGGTCAAGTACCTGGAGTT, 5′-TGAGCATCTGCTCCAAAGTC; *Pdk4*, 5′-CCGCTGTCCATGAAGCA, 5′-GCAGAAAAGCAAAGGACGTT; *Cycs*, 5′-ACCAAATCTCCACGGTCTGTT, 5′-GGATTCTCCAAATACTCCATCAG; *Lpl*, 5′-TTTGTGAAATGCCATGACAAG, 5′-CAGATGCTTTCTTCTCTTGTTTGT; *Ldha*, 5′-TGCCTACGAGGTGATCAAGCT, 5′-GCACCCGCCTAAGGTTCTTC; *Ldhb*, 5′-AGTCTCCCGTGCATCCTCAA, 5′-AGGGTGTCCGCACTCTTCCT; *Ppargc1a*, 5′-CGGAAATCATATCCAACCAG, 5′-TGAGAACCGCTAGCAAGTTTG; *Ppargc1b*, 5′-TCCAGAAGTCAGCGGCCT, 5′-CTGAGCCCGCAGTGTGG; *Esrra*, 5′-AGGAGTACGTCCTGCTG, 5′-CCTCAGCATCTTCAATG; *Esrrb*, 5′-ACGGCTGGATTCGGAGAAC, 5′-TCCTGCTCAACCCCTAGTAGATTC; *Esrrg*, 5′-TGACTTGGCTGACCGAG, 5′-CCGAGGATCAGAATCTCC; *Ppara*, 5′-ACTACGGAGTTCACGCATGTG, 5′-TTGTCGTACACCAGCTTCAGC; *Ppard*, 5′-GTATGCGCATGGGACTCAC, 5′-GTCTGAGCGCAGATGGACT; *Myh7*, 5′-GCCAACTATGCTGGAGCTGATGCCC, 5′-GGTGCGTGGAGCGCAAGTTTGTCATAAG; *Myh1*, 5′-GGCAGCAGCAGCTGCGGAAGCAGAGTCTGG, 5′-GAGTGCTCCTCAGATTGGTCATTAGC; *Myh2*, 5′-GGCACAAACTGCTGAAGCAGAGGC, 5′-GGTGCTCCTGAGGTTGGTCATCAGC; *Myh4*, 5′-GAGCTACTGGATGCCAGTGAGCGC, 5′-CTGGACGATGTCTTCCATCTCTCC. For human gene: *LDHB*, 5′-GATGGATTTTGGGGGAACAT, 5′-AACACCTGCCACA-

TTCACAC; and *PPARGC1A*, 5′-TGAGAGGGCCAAGCAAAG, 5′-ATAAATCACACGGCGCTCTT.

Mitochondrial DNA Analyses—Genomic/mitochondrial DNA was measured as described previously (37). Mitochondrial DNA content was determined by SYBR Green analysis (Takara Bio). The levels of NADH dehydrogenase subunit 1 (mitochondrial DNA) were normalized to the levels of lipoprotein lipase (genomic DNA).

Antibodies and Immunoblotting Studies—Antibodies directed against MHC1 (BA-D5) and MHC2b (BF-F3) were purchased from the Developmental Studies Hybridoma Bank; antibodies directed against cytochrome *c* (bs1089) and α-tubulin (bs1699) antibody were from Bioworld; anti-myoglobin (sc-25607) was from Santa Cruz; anti-FLAG M2 (F1804) was from Sigma; anti-Atpb (ab14730) was from Abcam; anti-Atp5a1 (14676–1-AP), anti-Cox4 (11242–1-AP), and anti-Sdha (14865–1-AP) were from Proteintech. Western blotting studies were performed as previously described (18, 19).

LDH Isoenzyme Analysis and Activity Assay—LDH isoenzyme patterns were determined as previously described (18). Five major LDH isoenzymes are found, because Ldhb polypeptide has more acidic amino acid residues than the Ldha polypeptide; thus the electrophoretic mobilities of the LDH isoenzymes migrate toward the positive electrode end as follows: LDH 1 > LDH 2 > LDH 3 > LDH 4 > LDH 5. Briefly, primary skeletal myotubes or mouse skeletal muscle were homogenized in a solution of 0.9% NaCl, 5 mM Tris-HCl, pH 7.4, and the lysates were centrifuged for 30 min at 15,000 × *g* to remove the cellular debris. 100 μg of protein/lane was loaded onto a 6% nondenaturing polyacrylamide gel. Following electrophoresis, the gel was placed in 10 ml of staining solution containing 0.1 M sodium lactate, 1.5 mM NAD, 0.1 M Tris-HCl (pH 8.6), 10 mM NaCl, 5 mM $MgCl_2$, 0.03 mg/ml phenazinmethosulphate, and 0.25 mg/ml nitro blue tetrazolium. Protein extracted from mouse heart served as a positive control. Total LDH activity and specific LDH activities (pyruvate to lactate conversions) were determined using the LDH assay kit (Nanjing Jiancheng Bioengineering Institute, A020-2) and (Beijing Leagene Biotechnology, TE0155) according to the manufacturer's protocol, respectively. Changes in absorbance were determined with a VersaMax ELISA microplate reader (Molecular Devices) at 450 nm for total LDH activity and 340 nm for LDH-mediated pyruvate to lactate conversion assay.

Lactate Concentration Measurement—Cell culture medium was collected. Lactate concentration was then determined with a VersaMax ELISA Microplate Reader (Molecular Devices) using the lactic acid assay kit (Nanjing Jiancheng Bioengineering Institute) according to the manufacturer's protocol.

Cell Culture—Primary muscle cells were isolated from skeletal muscles as previously described (18, 19). For differentiation, the cells were washed with PBS, refed with 2% horse serum/DMEM differentiation medium, and refed daily. The cells were then differentiated for 3 days prior to harvest. Primary myoblasts were infected with an adenovirus overexpressing GFP or PGC-1α as previously described (18, 19). 12 h postinfection, the cells were induced to differentiation for 3 days.

Oxygen Consumption Measurements—Cellular OCRs were measured using the XF24 analyzer (Seahorse Bioscience Inc.) per the manufacturer's protocol. The basal OCR was first measured in XF assay medium without sodium pyruvate, followed by administration of 10 mM sodium pyruvate. Uncoupled respiration was evaluated following the addition of oligomycin (2 μM) to inhibit ATP synthase by addition of the uncoupler FCCP (2 μM) and then followed by the addition of rotenone/antimycin (1 μM). Immediately after measurement, total protein levels were measured with the Micro BCA protein assay kit (Thermo Scientific) for data correction.

Cell Transfection and Luciferase Reporter Assays—pcDNA3.1 and pcDNA3.1-PGC-1α vectors have been described previously (19). The mouse *Ldhb* gene promoter deletion series was generated by PCR amplification from C57BL/6J genomic DNA followed by cloning into the pGL3 Basic luciferase reporter plasmid using BglII and MluI sites. The following 5′ primers were used: 5′-CTGGCTGACCTAGATCTCCGTTTC (m*Ldhb*.Luc.1791), 5′-TGGATGAGACAAAGATCTAAGAATGTGG (m*Ldhb*.Luc.869), and 5′-GAGAGATCTTGCACACTCCAGCCTTG (m*Ldhb*.Luc.122). The same 3′ primer was used with all constructs: 5′-ACAACACACGCGTTGATGTTCAG. Site-directed mutagenesis was performed using complementary oligonucleotides as follows (with mutated nucleotides shown in lowercase): 5′-GTGCCTCAGCGGAgatctACCTCTAACTTTAG (ERRmut#1) and 5′-AAAGTTAGAGGTagatcTCCGCTGAGGCA (ERRmut#2). C2C12 cells were obtained from the American Type Culture Collection and were cultured at 37 °C and 5% CO_2 in Dulbecco's modified Eagle's medium supplemented with 10% fetal calf serum, 1,000 units/ml penicillin, and 100 μg/ml streptomycin. Transient transfections in C2C12 cells were performed using Attractene transfection reagent (Qiagen) as per the manufacturer's protocol. Briefly, 350 ng of reporter was cotransfected with 100 ng of nuclear receptor expression vectors and 25 ng of CMV promoter-driven *Renilla* luciferase to control for transfection efficiency. The cells were harvested 48 h after transfection. The luciferase assay was performed using Dual-Glo (Promega) according to the manufacturer's recommendations. All transfection data are presented as the means ± S.E. for at least three separate transfection experiments.

Statistical Analyses—All mouse and cell studies were analyzed by Student's *t* test or one-way analysis of variance coupled to a Fisher's least significant difference post hoc test when more than two groups were compared. The data represent the means ± S.E., with a statistically significant difference defined as a value of $p < 0.05$. Statistical analyses in human studies were performed using JMP 9.0.0 (SAS Institute Inc.), and values are presented as means ± S.E. Gene expression levels in human studies were analyzed using the Spearman correlation or Pearson correlation test. Significant differences were defined as $p < 0.05$.

Author Contributions—X. L. and L. L. contributed equally to this work and performed most of the experiments with assistance from T. F., Q. Z., D. Z., L. X., J. L., Y. K., H. X., F. Y., and L .L., whereas R. B. V. and D. P. K. contributed reagents and provided scientific insight and discussion. S. R. S. was the principal investigator responsible for the clinical studies. Z. G. provided oversight of the study including experimental design and data interpretation and wrote the manuscript. All authors reviewed and contributed to the manuscript.

Acknowledgments—We give special thanks to Dr. Jiansheng Kang (Shanghai Institute for Biological Sciences), Dr. Bin Lv (Wenzhou Medical University), and Dr. Su-neng Fu (Tsinghua University) for ETC antibodies.

References

1. Burke, L. M., and Hawley, J. A. (1999) Carbohydrate and exercise. *Curr. Opin. Clin. Nutr. Metab. Care* **2,** 515–520
2. Coggan, A. R. (1991) Plasma glucose metabolism during exercise in humans. *Sports Med.* **11,** 102–124
3. Hargreaves, M. (2004) Muscle glycogen and metabolic regulation. *Proc. Nutr. Soc.* **63,** 217–220
4. Hawley, J. A. (2002) Adaptations of skeletal muscle to prolonged, intense endurance training. *Clin. Exp. Pharmacol. Physiol.* **29,** 218–222
5. Holloszy, J. O., Kohrt, W. M., and Hansen, P. A. (1998) The regulation of carbohydrate and fat metabolism during and after exercise. *Front. Biosci.* **3,** D1011–D1027
6. Booth, F. W., and Thomason, D. B. (1991) Molecular and cellular adaptation of muscle in response to exercise: perspectives of various models. *Physiol. Rev.* **71,** 541–585
7. Neufer, P. D., Bamman, M. M., Muoio, D. M., Bouchard, C., Cooper, D. M., Goodpaster, B. H., Booth, F. W., Kohrt, W. M., Gerszten, R. E., Mattson, M. P., Hepple, R. T., Kraus, W. E., Reid, M. B., Bodine, S. C., Jakicic, J. M., *et al.* (2015) Understanding the cellular and molecular mechanisms of physical activity-induced health benefits. *Cell Metab.* **22,** 4–11
8. Rowe, G. C., Safdar, A., and Arany, Z. (2014) Running forward: new frontiers in endurance exercise biology. *Circulation* **129,** 798–810
9. Zierath, J. R., and Hawley, J. A. (2004) Skeletal muscle fiber type: influence on contractile and metabolic properties. *PLoS Biol.* **2,** e348
10. Yan, Z., Okutsu, M., Akhtar, Y. N., and Lira, V. A. (2011) Regulation of exercise-induced fiber type transformation, mitochondrial biogenesis, and angiogenesis in skeletal muscle. *J. Appl. Physiol.* **110,** 264–274
11. Egan, B., and Zierath, J. R. (2013) Exercise metabolism and the molecular regulation of skeletal muscle adaptation. *Cell Metab.* **17,** 162–184
12. Holloszy, J. O., and Coyle, E. F. (1984) Adaptations of skeletal muscle to endurance exercise and their metabolic consequences. *J. Appl. Physiol. Respir. Environ. Exerc. Physiol.* **56,** 831–838
13. Liu, J., Liang, X., and Gan, Z. (2015) Transcriptional regulatory circuits controlling muscle fiber type switching. *Sci. China Life Sci.* **58,** 321–327
14. Mujika, I., and Padilla, S. (2001) Muscular characteristics of detraining in humans. *Med. Sci. Sports Exerc.* **33,** 1297–1303
15. Hagberg, J. M., Seals, D. R., Yerg, J. E., Gavin, J., Gingerich, R., Premachandra, B., and Holloszy, J. O. (1988) Metabolic responses to exercise in young and older athletes and sedentary men. *J. Appl. Physiol.* **65,** 900–908
16. Cairns, S. P. (2006) Lactic acid and exercise performance: culprit or friend? *Sports Med.* **36,** 279–291
17. Arany, Z., He, H., Lin, J., Hoyer, K., Handschin, C., Toka, O., Ahmad, F., Matsui, T., Chin, S., Wu, P. H., Rybkin, I. I., Shelton, J. M., Manieri, M., Cinti, S., Schoen, F. J., *et al.* (2005) Transcriptional coactivator PGC-1α controls the energy state and contractile function of cardiac muscle. *Cell Metab.* **1,** 259–271
18. Gan, Z., Burkart-Hartman, E. M., Han, D. H., Finck, B., Leone, T. C., Smith, E. Y., Ayala, J. E., Holloszy, J., and Kelly, D. P. (2011) The nuclear receptor PPARβ/δ programs muscle glucose metabolism in cooperation with AMPK and MEF2. *Genes Dev.* **25,** 2619–2630
19. Gan, Z., Rumsey, J., Hazen, B. C., Lai, L., Leone, T. C., Vega, R. B., Xie, H., Conley, K. E., Auwerx, J., Smith, S. R., Olson, E. N., Kralli, A., and Kelly, D. P. (2013) Nuclear receptor/microRNA circuitry links muscle fiber type to energy metabolism. *J. Clin. Invest.* **123,** 2564–2575
20. Narkar, V. A., Downes, M., Yu, R. T., Embler, E., Wang, Y. X., Banayo, E., Mihaylova, M. M., Nelson, M. C., Zou, Y., Juguilon, H., Kang, H., Shaw, R. J., and Evans, R. M. (2008) AMPK and PPARδ agonists are exercise mimetics. *Cell* **134,** 405–415
21. Narkar, V. A., Fan, W., Downes, M., Yu, R. T., Jonker, J. W., Alaynick, W. A., Banayo, E., Karunasiri, M. S., Lorca, S., and Evans, R. M. (2011) Exercise and PGC-1α-independent synchronization of type I muscle metabolism and vasculature by ERRγ. *Cell Metab.* **13,** 283–293
22. Rangwala, S. M., Wang, X., Calvo, J. A., Lindsley, L., Zhang, Y., Deyneko, G., Beaulieu, V., Gao, J., Turner, G., and Markovits, J. (2010) Estrogen-related receptor γ is a key regulator of muscle mitochondrial activity and oxidative capacity. *J. Biol. Chem.* **285,** 22619–22629
23. Wang, Y. X., Zhang, C. L., Yu, R. T., Cho, H. K., Nelson, M. C., Bayuga-Ocampo, C. R., Ham, J., Kang, H., and Evans, R. M. (2004) Regulation of muscle fiber type and running endurance by PPARδ. *PLoS Biol.* **2,** e294
24. Zechner, C., Lai, L., Zechner, J. F., Geng, T., Yan, Z., Rumsey, J. W., Collia, D., Chen, Z., Wozniak, D. F., Leone, T. C., and Kelly, D. P. (2010) Total skeletal muscle PGC-1 deficiency uncouples mitochondrial derangements from fiber type determination and insulin sensitivity. *Cell Metab.* **12,** 633–642
25. Lin, J., Wu, H., Tarr, P. T., Zhang, C. Y., Wu, Z., Boss, O., Michael, L. F., Puigserver, P., Isotani, E., Olson, E. N., Lowell, B. B., Bassel-Duby, R., and Spiegelman, B. M. (2002) Transcriptional co-activator PGC-1 α drives the formation of slow-twitch muscle fibres. *Nature* **418,** 797–801
26. Seiler, S. E., Koves, T. R., Gooding, J. R., Wong, K. E., Stevens, R. D., Ilkayeva, O. R., Wittmann, A. H., DeBalsi, K. L., Davies, M. N., Lindeboom, L., Schrauwen, P., Schrauwen-Hinderling, V. B., and Muoio, D. M. (2015) Carnitine acetyltransferase mitigates metabolic inertia and muscle fatigue during exercise. *Cell Metab.* **22,** 65–76
27. Muoio, D. M., Noland, R. C., Kovalik, J. P., Seiler, S. E., Davies, M. N., DeBalsi, K. L., Ilkayeva, O. R., Stevens, R. D., Kheterpal, I., Zhang, J., Covington, J. D., Bajpeyi, S., Ravussin, E., Kraus, W., Koves, T. R., *et al.* (2012) Muscle-specific deletion of carnitine acetyltransferase compromises glucose tolerance and metabolic flexibility. *Cell Metab.* **15,** 764–777
28. Juel, C., and Halestrap, A. P. (1999) Lactate transport in skeletal muscle: role and regulation of the monocarboxylate transporter. *J. Physiol.* **517,** 633–642
29. Jorfeldt, L., and Wahren, J. (1970) Human forearm muscle metabolism during exercise: V. quantitative aspects of glucose uptake and lactate production during prolonged exercise. *Scand. J. Clin. Lab. Invest.* **26,** 73–81
30. Omachi, A., and Lifson, N. (1956) Metabolism of isotopic lactate by the isolated perfused dog gastrocnemius. *Am. J. Physiol.* **185,** 35–40
31. Cahn, R. D., Zwilling, E., Kaplan, N. O., and Levine, L. (1962) Nature and development of lactic dehydrogenases: the two major types of this enzyme form molecular hybrids which change in makeup during development. *Science* **136,** 962–969
32. Dawson, D. M., Goodfriend, T. L., and Kaplan, N. O. (1964) Lactic dehydrogenases: functions of the two types rates of synthesis of the two major forms can be correlated with metabolic differentiation. *Science* **143,** 929–933
33. Draoui, N., and Feron, O. (2011) Lactate shuttles at a glance: from physiological paradigms to anti-cancer treatments. *Dis. Model. Mech.* **4,** 727–732
34. Van and Hall, G. (2000) Lactate as a fuel for mitochondrial respiration. *Acta Physiol. Scand.* **168,** 643–656
35. Markert, C. L., Shaklee, J. B., and Whitt, G. S. (1975) Evolution of a gene: multiple genes for LDH isozymes provide a model of the evolution of gene structure, function and regulation. *Science* **189,** 102–114
36. Pesce, A., McKay, R. H., Stolzenbach, F., Cahn, R. D., and Kaplan, N. O. (1964) The comparative enzymology of lactic dehydrogenases: I. properties of the crystalline beef and chicken enzymes. *J. Biol. Chem.* **239,** 1753–1761
37. Liu, J., Liang, X., Zhou, D., Lai, L., Xiao, L., Liu, L., Fu, T., Kong, Y., Zhou, Q., Vega, R. B., Zhu, M. S., Kelly, D. P., Gao, X., and Gan, Z. (2016) Coupling of mitochondrial function and skeletal muscle fiber type by a miR-499/Fnip1/AMPK circuit. *EMBO Mol. Med.* **8,** 1212–1228
38. Summermatter, S., Santos, G., Pérez-Schindler, J., and Handschin, C. (2013) Skeletal muscle PGC-1α controls whole-body lactate homeostasis through estrogen-related receptor α-dependent activation of LDH B and repression of LDH A. *Proc. Natl. Acad. Sci. U.S.A.* **110,** 8738–8743
39. Costford, S. R., Bajpeyi, S., Pasarica, M., Albarado, D. C., Thomas, S. C., Xie, H., Church, T. S., Jubrias, S. A., Conley, K. E., and Smith, S. R. (2010) Skeletal muscle NAMPT is induced by exercise in humans. *Am. J. Physiol. Endocrinol. Metab.* **298,** E117–E126
40. Bajpeyi, S., Pasarica, M., Moro, C., Conley, K., Jubrias, S., Sereda, O., Burk, D. H., Zhang, Z., Gupta, A., Kjems, L., and Smith, S. R. (2011) Skeletal

muscle mitochondrial capacity and insulin resistance in type 2 diabetes. *J. Clin. Endocrinol. Metab.* **96,** 1160–1168

41. Knight, D. R., Poole, D. C., Schaffartzik, W., Guy, H. J., Prediletto, R., Hogan, M. C., and Wagner, P. D. (1992) Relationship between body and leg VO2 during maximal cycle ergometry. *J. Appl. Physiol.* **73,** 1114–1121
42. Schiaffino, S., and Reggiani, C. (2011) Fiber types in mammalian skeletal muscles. *Physiol. Rev.* **91,** 1447–1531
43. Elustondo, P. A., White, A. E., Hughes, M. E., Brebner, K., Pavlov, E., and Kane, D. A. (2013) Physical and functional association of lactate dehydrogenase (LDH) with skeletal muscle mitochondria. *J. Biol. Chem.* **288,** 25309–25317
44. Hashimoto, T., Hussien, R., Oommen, S., Gohil, K., and Brooks, G. A. (2007) Lactate sensitive transcription factor network in L6 cells: activation of MCT1 and mitochondrial biogenesis. *FASEB J.* **21,** 2602–2612
45. Li, S., Swanson, S. K., Gogol, M., Florens, L., Washburn, M. P., Workman, J. L., and Suganuma, T. (2015) Serine and SAM responsive complex SESAME regulates histone modification crosstalk by sensing cellular metabolism. *Mol. Cell* **60,** 408–421
46. Apple, F. S., and Rogers, M. A. (1986) Skeletal muscle lactate dehydrogenase isozyme alterations in men and women marathon runners. *J. Appl. Physiol.* **61,** 477–481
47. Hittel, D. S., Kraus, W. E., Tanner, C. J., Houmard, J. A., and Hoffman, E. P. (2005) Exercise training increases electron and substrate shuttling proteins in muscle of overweight men and women with the metabolic syndrome. *J. Appl. Physiol.* **98,** 168–179
48. Martin, O. J., Lai, L., Soundarapandian, M. M., Leone, T. C., Zorzano, A., Keller, M. P., Attie, A. D., Muoio, D. M., and Kelly, D. P. (2014) A role for peroxisome proliferator-activated receptor γ coactivator-1 in the control of mitochondrial dynamics during postnatal cardiac growth. *Circ. Res.* **114,** 626–636